# Tuned Mass Dampers for Improving the Sustainability and Resilience of Seven Reinforced Concrete Chimneys Under Environmental Loads


## Abstract

Since the fifties of the twenty century, new manufacturing and chemical plants have employed reinforced concrete (RC) to build chimneys, stimulated by industrial developments and environmental requirements. Many RC chimneys were designed and constructed without specific earthquake-resistance provisions. Under seismic loads, chimneys are characterized by inelastic response leading to potential brittle collapse. The construction of new chimneys is not an attractive solution in terms of construction time and, in several cases, the need to change the plant layout. Historical chimneys represent a symbol of important industrial plants, representative for the community that has grown around it. In addition, the current call for sustainability highlights the importance of material recycling. Retrofitting existing chimneys to improve resilience and ability to survive under environmental conditions is an acceptable approach for the development. This paper investigates the seismic performance of seven RC chimneys, originally designed in absence of seismic action, equipped with Tuned Mass Dampers (TMDs). The nonlinear material properties of concrete and steel rebars are considered to optimize the TMDs performance, by conducting time-history dynamic analyses under five European earthquakes. The parameters of the TMDs are optimized and the performance of the system is investigated: the capability of the TMDs is assessed in reducing top displacements, base shear and base moment. The additional equivalent damping and the change in vibrational modes, in terms of frequencies and participating masses, are evaluated as well. A parametric study is conducted to understand the influence of geometrical slenderness, taper ratio, height and vertically distributed mass, on chimneys response to earthquakes, including dimensionless parameters related to top displacement, base shear and base moment. Among the geometrical parameters here investigated, geometrical slenderness is predominant with respect to the others, afflicting the mass ratio and consequently the optimized parameters of the TMDs, the base shear and base moment. The geometrical features seem to not influence the equivalent damping that depends much more on the frequency of the original chimney. In addition, an energy balance is performed to assess the energy dissipated by TMDs. When TMDs are present, the damping energy of the chimneys increases with respect to the decrease of the kinetic and inelastic energies.



***Keywords***: *Environmental loads, sustainability, tuned mass damper, reinforced concrete, chimney, seismic response, non-linear analysis.*


## 1. Introduction

**Background**: All over the world, many industrial plants rely on chimneys as a vital element for the exhaust of combustion gases and pollution dispersion. As a monumental symbol of the industrialization era, older chimneys are in many places of the world. Since the fifties of the twenty century, new manufacturing and chemical plants employed reinforced concrete (RC), instead of traditional masonry, to build chimneys stimulated by industrial developments and environmental requirements. Older industrial chimneys built between the end of the nineteenth century and the beginning of the twentieth century are mostly masonry [1], [2]. Chimneys are fundamental for combustion gases discharge and achieving the necessary “chimney effect” for industrial processes [3]. Masonry chimneys consist of three main parts: base, shaft with “single skin” or “double skins,” and ornamental crown, characterized by a hollow circular section and a maximum height of about 25-30 m [4], [5]. These masonry chimneys were replaced by RC ones, with significantly different configurations and structural characteristics. Due to advances in materials and concrete production

techniques, it was possible to satisfy the essential industrial requirements with a reduced environmental impact. RC enabled the building of chimneys with a significant increase in height (up to 400 m). Chimneys ranging between 100 m and 400 m in height were built. For instance, the chimney in Pitesti, Romania, and the chimney in Torrevaldaliga-Civitavecchia, close to Rome.

**Seismic performance of RC chimneys:** An important aim in the existing RC structures is to limit the negative impact of vibrations [6]. Many RC chimneys were designed and constructed without specific earthquake-resistance provisions, considering only the wind as the dominant lateral design load [7]. In some European countries, for example in Italy, many chimneys were built in areas that nowadays are considered seismic zones [8]. There is evidence of structural negligence of the seismic performance of many existing RC chimneys, in terms of resilience, ductility, and economic aspects. Therefore, historical chimneys, including those that are not in use, should be safeguarded as they represent the important industrial heritage of the local community, and they serve as an entrepreneurial symbol. Also, the structural behavior of RC chimneys, currently in areas classified as seismic zones, should be improved to avoid potential collapse, threatening human safety, and interrupting industrial production with substantial economic losses (such as the Izmit Tupras Refinery accident in 1999). Under seismic loads, chimneys are characterized by their inelastic response, different from the elastic behavior of tall buildings under service wind loads. Higher vibration modes and longer periods of oscillations drive a complex global dynamic response under earthquake loads. This can lead to a significant increase in structural stress states, with a potential for brittle collapse [4,9–15].

A recent study reported six major chimney failures, out of 739 chimneys that were investigated [16]. The damage to these RC chimneys was mainly caused by seismic and wind actions, temperature-induced stress, and construction defects [14]. On the other hand, the behavior of RC structures subjected to dynamic loads is also influenced by important physical parameters as described in [17].

Several research studies deepen the analysis of fracture processes in RC structures [18][19][20][21] and reveal the crack pattern in slender constructions due to seismic loads [22,23]. In particular, a failure-prone region between 30% to 80% of the height of a standard designed chimney was identified. This zone experiences inelastic deformations. Failures may occur in the lateral, vertical, and inclined directions, after strong earthquakes. Predominant cracks with 20–30 mm width were observed after seismic events [16]. A specific design for wind may not allow for adequate resilience under seismic loads. This is because the design for wind demands higher stiffness and higher strength. A design with lower stiffness and higher ductility is favorable under seismic action [22], [24]. The increase in height over 130 m exposes chimneys to large displacements, causing cracks that demand extensive rehabilitation. Moreover, the radius to thickness ratio has a relevant influence on the dynamic response. The displacement decreases with the increase in the radius to thickness ratio. Chimneys tapered from bottom to top experience lower displacements, compared to those that are tapered from the bottom and become uniform at one third of the total height. The shell stress decreases with the increase in the radius to thickness ratio, for a fully tapered chimney, compared to a partially tapered one. Additionally, for a higher radius to thickness ratio, there is a decrease in the total base shear force [25]. For improving the seismic response of chimneys, adequate modeling of the structure is indispensable [14,15]. In addition, passive tuned mass dampers play a vital role in response reduction, while presenting a cost-effective solution [26].

**Paper layout:** The construction of new chimneys, instead of the seismic retrofitting of existing ones, is not an attractive solution, in terms of construction time, and sometimes the need to change the plant layout. In addition, the current call for sustainability highlights the importance of material recycling and improved designs [27–30]. Retrofitting existing structures, to improve their resilience and hence the ability to survive under environmental conditions, is ultimately an acceptable approach for the development while preserving the environment under the sustainability constraints. This paper investigates the seismic performance of seven existing RC chimneys equipped by tuned mass dampers (TMDs) under five seismic events. The seismic response of the chimneys with and without TMDs is

obtained by performing nonlinear dynamic analyses. The paper layout is as follows. Section 2 presents an overview of the use of tuned mass dampers for the seismic retrofitting of chimneys. Section 3 provides the structural characteristics of the chimneys investigated in this paper. The finite element analysis is presented in Section 4. In Section 5, the optimal parameters of the TMDs are derived. The equivalent damping of the chimneys with TMDs is investigated in Section 6. The influence of the chimneys geometrical parameters (aspect and taper ratios) on the effectiveness of the TMDs is discussed in Section 7. An energy balance analysis is conducted in Section 8. Section 9 summarizes the main findings of the paper.

## 2. Tuned mass damper for seismic retrofitting of chimneys

Fig. 1. shows typical TMD installation on an existing RC chimney. TMDs and viscous dampers can protect buildings and other structures under seismic loads [31–43]. Several approaches can be generally considered to improve the seismic response of chimneys. In many countries, when the seismic improvement concerns a historical masonry chimney, the project lead should present the renovation plan to the department responsible for the environment and historical buildings. This step is necessary to ascertain that the renovation will preserve the original structure without modifying the essence of the chimney (i.e., the historical chimney could be a symbol of an important industrial plant) [44]. Some requirements are expressly indicated, such as the reversibility and the use of compatible materials. To fulfill these requirements, a TMD can be used to reduce the base shear, base moment, and top displacements [4]. This type of solution is usually considered to reduce the seismic and wind response of existing RC chimneys, by applying a single TMD or vertically distributed multiple mass dampers (m-TMDs) [9]. For the two configurations (TMD or m-TMDs), the energetic approach is pursued by increasing the structural damping and shifting the period of the new system represented by the chimney and the device [45]. Fig. 2 demonstrates the general benefits of the frequency shifting and the increased damping due to the installation of TMD. Compared to the primary structure alone, the new system (chimney with TMD) may have more structural damping and favorable period shift in the response spectrum curve, which reduces the seismic response. For RC chimneys, the use of TMDs represents a valid solution for improving the structural performance under horizontal loads, which increases the serviceability and availability of the chimney by maximizing its economic value related to the chemical processes of the plant. The choice of a TMD system should consider the material issues (state of concrete, conditions of reinforcing bars, etc.), the geometry, the location of the chimney and the plant layout. Special attention should be paid to the height of the chimney and the purpose of the renovation project in terms of the required percentage of performance improvement under seismic loads, wind loads or the combination of the two [46,47]. RC chimneys may experience a moderate ductile response under severe loading and unloading cycles due to yielding in the reinforcement bars. In many cases, a single TMD represents an acceptable solution in terms of structural and economic convenience.

**Fig. 1.** World record for a 41 *t* tuned mass damper installed on the top of a 180 m RC chimney [48].

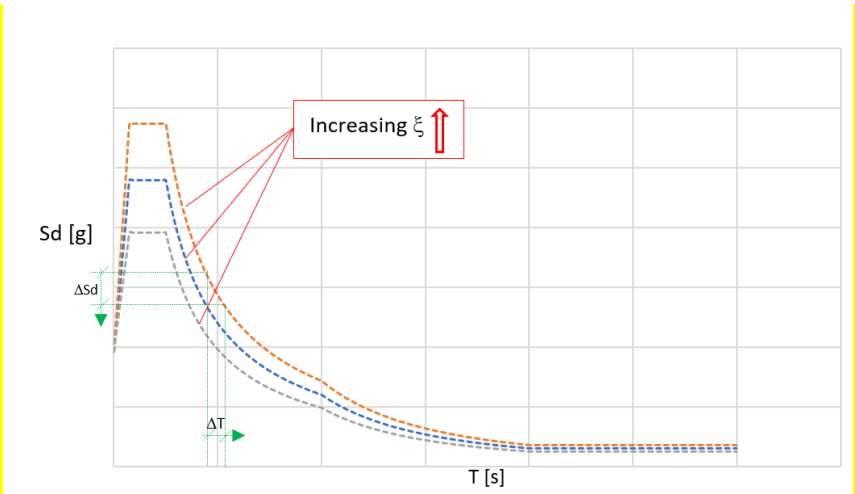


**Fig. 2.** Generic representation of the seismic benefits due to a TMD, i.e., increased damping and period shifting.

## 3. Characteristics of the seven RC chimneys

The structural configuration of the RC chimneys may change as a function of the height, location, and industrial needs. It is worth mentioning that some of the European RC chimneys built between 1950 and 1970 present inner pipes (also realized in steel and acid-resistant masonry) [49]. These inner pipes are located about 10 m apart and connected to the inner shell and outer skin. Fig. 3. represents an example of this configuration.

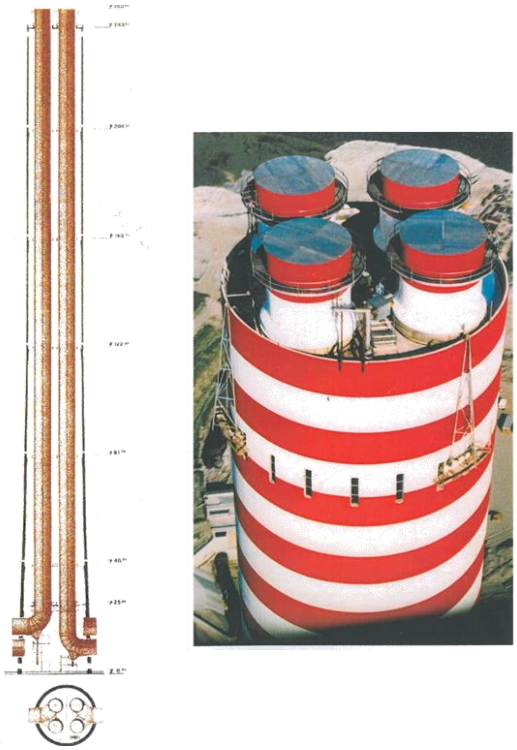

**Fig. 3.** A 245 m RC chimney located in Porto Tolle (Rovigo, Italy). Left: section and top view of the chimney. Right: a general view of the chimney.

The seven RC chimneys investigated in this study were built between 1960 and 1985 (Fig. 4). The case study chimneys are classified according to four main geometrical features: the height (H), the geometrical slenderness ratio that is the ratio between the maximum height and the outer diameter at the base (or $\lambda = H/D_{base}$), the taper ratio that is the ratio of the outer diameter at the top to the outer diameter at the base (or $t_d = D_{top}/D_{base}$), and the mass distribution along the height ($q_h$).

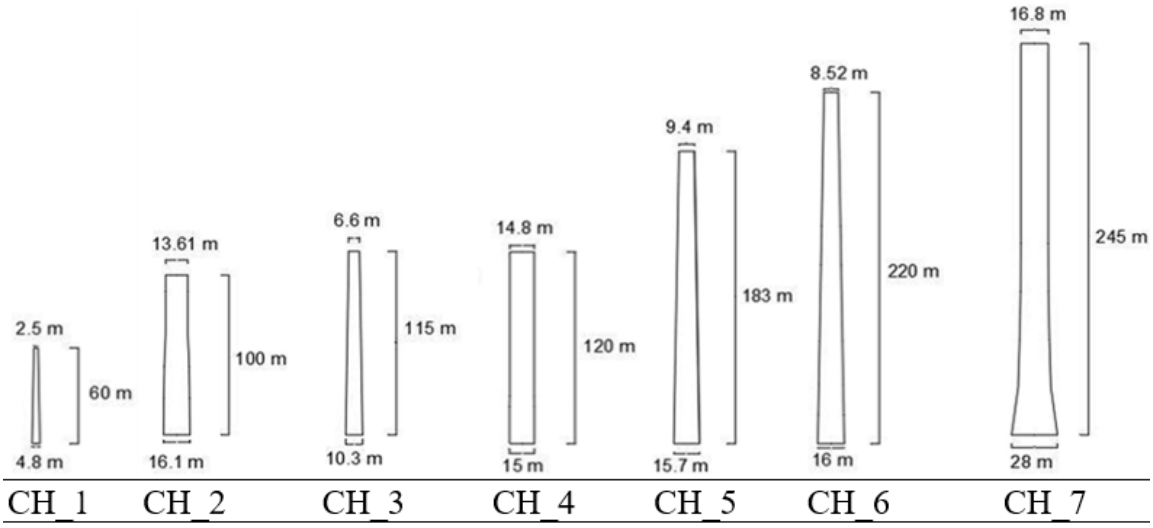


**Fig. 4.** Elevation view of the seven case study chimneys (each chimney is named as CH_number, see Table 1 for more details). Height, base diameter and top diameter are shown in m.

The characteristics of the chimneys are listed in Table 1. The general characteristics include the height (H), the outer base diameter ($D_{base}$), the outer top diameter ($D_{top}$), the taper ratio ($t_d$), the slenderness ratio ($\lambda$), the wall thickness ($t_h$), the type of concrete and steel used, and the location.

Table 1. Main characteristics of the seven case study chimneys.

| chimney | $D_{base}$, m | $D_{top}$, m | H, m | $t_d$ | $\lambda$ | $t_h$, cm | concrete | steel | $m_{tot}$ | $m_{genr}$ | location |
|---|---|---|---|---|---|---|---|---|---|---|---|
| CH_1 | 4.8 | 2.5 | 60 | 0.52 | 12.50 | 30 | C20/25 | Aq50 | 9302 | 192.6 | Senigallia, Italy |
| CH_2 | 16.1 | 13.6 | 100 | 0.85 | 6.21 | 40-30 | C35/45 | FeB44k | 47704.2 | 1055.9 | Panipat, India |
| CH_3 | 10.3 | 6.6 | 115 | 0.64 | 11.17 | 45-20 | C35/45 | FeB44k | 32041.7 | 546.5 | Turkey |
| CH_4 | 15.0 | 14.8 | 120 | 0.99 | 8.00 | 35-26.5 | C35/45 | FeB44k | 45564.3 | 1089 | Cagliari, Italy |
| CH_5 | 15.7 | 9.4 | 183 | 0.60 | 11.66 | 60-30 | C45/55 | FeB44k | 90299.1 | 1466.3 | Birmingham, UK |
| CH_6 | 16.0 | 8.5 | 220 | 0.53 | 13.75 | 76-20 | C35/45 | Aq50 | 140752 | 1647 | La Spezia, Italy |
| CH_7 | 26.0 | 16.8 | 245 | 0.65 | 9.42 | 70-35 | C35/45 | FeB44k | 168617 | 2926.2 | Italy |

Note: $D_{base}$= outer diameter at the base; $D_{top}$ = outer diameter at the top; H = height; $t_d$ = taper ratio; $\lambda$ = slenderness ratio; $t_h$ = wall thickness of the circular hollow section; $m_{tot}$ is the total mass in *t*; $m_{genr}$ is the generalized mass in *t*.

## 4. Finite element analysis (Phase A)

The finite element model (FEM) of each chimney was established in MIDAS Gen [50], by relying on detailed structural properties. Each FEM is characterized by vertically disposed beam elements; the node at the base of the chimney is fully constrained (fixed) (Fig. 5). The choice of discretizing by 10 elements also depends on calculation effort. However, the influence of a discretization by 100 beam elements was evaluated for two chimneys, chimney 1 and chimney 7. The differences in terms of vibration modes and masses involved are minimal, Table 4; however, the calculation effort is considerably greater. For a preliminary analysis, the mass ratio was set to zero. The design and the implementation of the TMD in the FEMs will be discussed in Section 5. The self-weight is defined by assigning the mechanical characteristics of the material, while the dead loads due to the inner structures and equipment are accounted for by considering distributed vertical beam load applied on the beam elements representing the chimney. The self-weight and the dead loads are converted to mass to carry out the finite element analysis for evaluating the periods of the structure, the equivalent participation mass, and the mode shapes. The nonlinear material behavior of concrete is accounted for by the Kent-Park property [51]. Similarly, the nonlinear properties of the steel rebars are considered [52]. The mechanical properties of the concrete and steel of the chimneys already indicated in Table 1 are listed in Table 2. The nonlinear properties are included in the model by fiber discretization of each section of the beam elements.

Table 2. Material mechanical properties.

| | concrete grade | | | steel grade | | |
|---|---|---|---|---|---|---|
| | C20/25 | C35/45 | C45/55 | grade | FeB 44K | Aq 50 |
| $f_c$ | 28750 | 45350 | 53650 | fy | 382610 | 234780 |
| $\varepsilon_0$ | 0.002 | 0.002 | 0.002 | $f_u$ | 440000 | 270000 |
| k | 1 | 1 | 1 | $E_s$ | 210000000 | 210000000 |
| z | 533.351 | 557.58 | 677.93 | $\varepsilon_{sh}$ | 0.02 | 0.02 |
| $\varepsilon_u$ | 0.00351 | 0.00417 | 0.00417 | $\varepsilon_{su}$ | 0.11 | 0.13 |

Note: stress and elastic modulus in $kN/m^2$

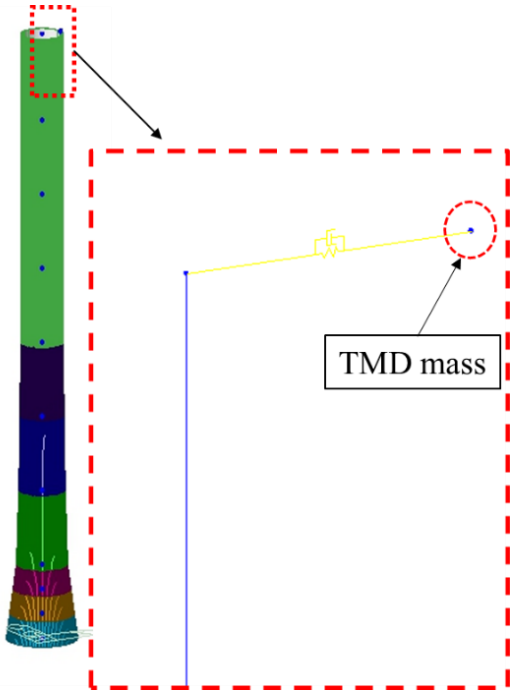


**Fig. 5.** A schematic representation of a TMD in the finite element model (FEM).

It is worth mentioning that the nonlinear normal modes represent the analogue of linear normal modes for nonlinear systems. Although the nonlinear normal modes do not have some of the key mathematical properties of linear normal modes (such as orthogonality), they share a number of important similarities and proved useful to explain the nonlinear phenomena. [53–55]. The fundamental period ($T_1$) and the corresponding modal participation mass ($M_1$) of the first mode, for each chimney, are obtained from the finite element analysis as listed in Table 3. Fig. 6 shows the mass participation of the first vibrational mode, the dominant period, and the corresponding dominant natural frequency of the seven chimneys as a function of the mass ratio (μ) of the TMD that will be discussed later. A mass ratio of zero means that the primary structure is without the TMD and should yield the results listed in Table 3.

Table 3. Finite element analysis results.

| chimney | $T_1$ [s] | $M_1$ [%] |
|---|---|---|
| CH_1 | 1.63 | 58.48 |
| CH_2 | 0.92 | 66.51 |
| CH_3 | 1.77 | 54.24 |
| CH_4 | 1.33 | 63.82 |
| CH_5 | 2.55 | 53.87 |
| CH_6 | 3.21 | 48.02 |
| CH_7 | 3.79 | 45.23 |

Table 4. Comparison between Chimney 1(CH 1) and Chimney 7 (CH 7) models in terms of vibrational modes and masses by adopting 10 (D1) and 100 (D2) discretizing elements.

| | Chimneys | | | |
|---|---|---|---|---|
| | CH_1_D1 | CH_1_D2 | CH_7_D1 | CH_7_D2 |
| Period | 1.632 | 1.629 | 3.794 | 3.791 |
| | Mass Participation | | | |
| 1st / 2nd | 58.48 | 57.95 | 44.23 | 43.36 |
| 3rd / 4th | 21.069 | 20.51 | 19.68 | 19.22 |
| 5th / 6th | 8.867 | 8.69 | 10.17 | 7.39 |

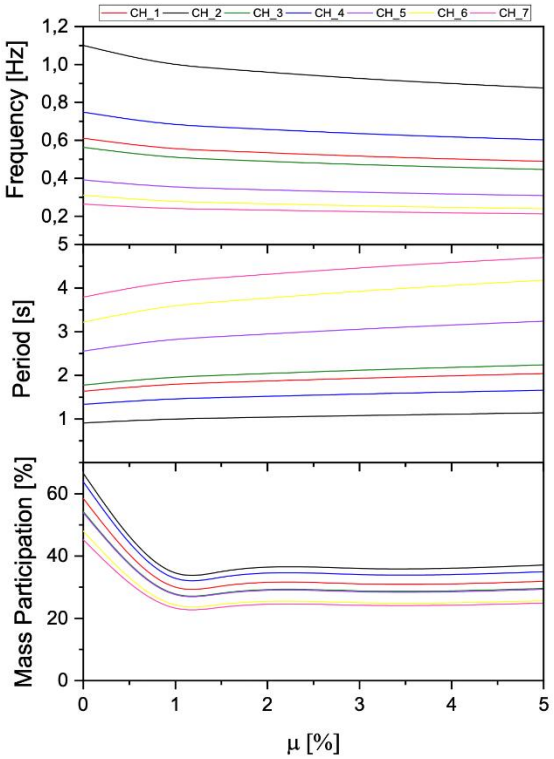


**Fig. 6.** Effect of the TMD mass ratio (μ) on the mass participation of the first vibrational mode, the natural period and the natural frequency.

It is worth mentioning that the mass participation of the first modes for the seven chimneys varies between 40% and 65% and the first vibrational period is in the range of 1 to 5 s. The influence of these parameters on the behavior of the chimneys under seismic action, as well as the capability of the TMDs to enhance the performance, will be investigated later.

## 5. Optimum parameters of the TMD (Phase B)

Once the vibration mode shapes and the main frequencies of the chimneys are known, the parameters of the TMDs can be estimated [56,57]. The seismic response can be analyzed by implementing the TMD in the FEM of each chimney. The TMD is implemented via a nodal mass connected to the chimney with spring and linear dashpot characterized by a stiffness ($k_{tmd}$) and damping coefficient ($c_{tmd}$). The boundary conditions of the node representing the TMD are set to allow for only the horizontal displacements of the mass (Fig. 5). The horizontal stiffness ($k_{tmd}$) and the related damping coefficient ($c_{tmd}$) are evaluated from the following relations [58], [59]:

$$k_{tmd} = \mu\, m\, \rho_{opt}^2\, \omega_s^2 \ , \tag{1}$$

$$c_{tmd} = 2\, \xi_{opt} \sqrt{(k_{tmd}\, \mu\, m)} \ , \tag{2}$$

$$\mu = \frac{m_d}{m} \ , \tag{3}$$

$$\rho_{opt} = \left(\frac{\sqrt{1-0.5\mu}}{1+\mu} + \sqrt{1-2\xi^2} - 1\right) - \left(2.375 - 1.034\sqrt{\mu} - 0.426\mu\right) \xi\, \mu - \left(3.730 - 16.903\sqrt{\mu} + 20.496\mu\right) \cdot \xi^2 \cdot \sqrt{\mu} \ , \tag{4}$$

$$\xi_{opt} = \sqrt{\left(\frac{\sqrt{3\mu}}{8(1+\mu)(1-0.5\mu)}\right)} + (0.151\xi - 0.175\xi^2) + (0.163\xi + 4.98\xi^2)\, \mu \ , \tag{5}$$

here $\mu$ is the mass ratio, $m$ is the mass of the chimney, $m_d$ is the mass of the TMD, $\omega_s$ is the dominant frequency of the chimney, $\rho_{opt}$ is the optimal frequency ratio, $\xi_{opt}$ is the optimal equivalent damping ratio, and $\xi$ is the equivalent structural damping ratio (without TMD). The mass ratio, $\mu$, of the TMD was considered to vary between 1% and 5%. The effect of the TMD mass ratio change on the characteristics of the chimneys, including the mass participation of the first vibrational mode, the natural period and the natural frequency, is shown in Fig. 6. It is worthy to mention that the first and the second vibrational modes are characterized by the same percentage of participating mass and by the same value of the natural frequency. By considering different values of the TMD mass, the seismic response of the "chimney with TMD" can be estimated using the FEM, where the seismic action is introduced using five acceleration times histories (Greece, Amatrice, L'Aquila, Friuli, and Montenegro), as shown in Fig. 7. The dominant characteristics of the seismic inputs are shown in Table 5. The seismic inputs have been selected to obtain a magnitude between 6 and 6.9 and a PGA value between 0.35 g and 0.53 g. However, they are characterized by different integral parametric values, gaining a large variability of the ground motion characteristics (Fig. 7) and Table 5, [60,61].

Table 5. Characteristics of the seismic inputs.

| event name | event ID | station | year | PGA [g] | PGV [cm/s] | PGD [cm] | magnitude | arias intensity [cm/s] |
|---|---|---|---|---|---|---|---|---|
| Friuli (Acc1) | IT-1976-0030 | FRC | 1976 | 0.35 | 23.7 | 5.3 | 6 | 84.5 |
| Montenegro (Acc2) | ME-1979-0003 | PETO | 1979 | 0.45 | 38.5 | 6.9 | 6.9 | 455.7 |
| Amatrice (Acc3) | EMSC-20161030_0000029 | AMT | 2016 | 0.53 | 37.9 | 7.5 | 6.5 | 156.4 |
| Greece (Acc4) | GR-1995-0047 | AIGA | 1995 | 0.52 | 51.3 | 8.3 | 6.5 | 117.1 |
| L'Aquila (Acc5) | IT-2009-0009 | AQG | 2009 | 0.49 | 35.8 | 6.0 | 6.1 | 132.4 |

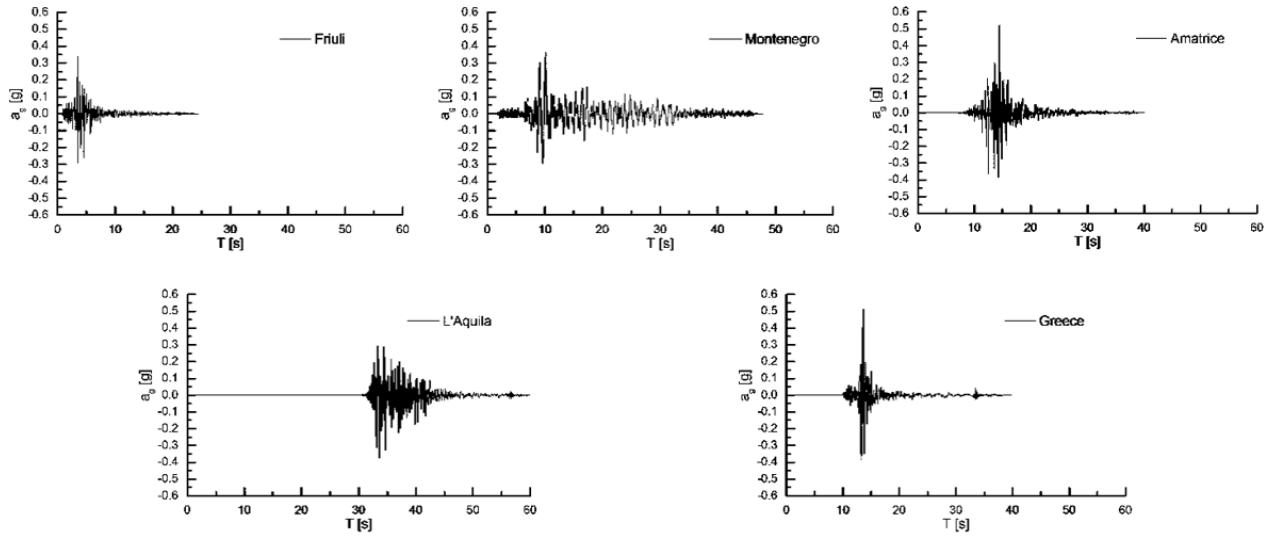


**Fig. 7.** Five different seismic motions: Friuli (Acc1), Montenegro (Acc2), Amatrice (Acc3), Greece (Acc4) and L'Aquila (Acc5).

Under the five ground motions, three fundamental responses are evaluated. The responses include the top displacement (η), the base shear (V), and the base moment (M). The performance criteria are defined as the change in these responses when the TMD is installed: Δη%, ΔV%, and ΔM%. The best TMD mass ratio, within the range of 1% to 5%, is obtained by maximizing the reductions in top displacement Δη%, base shear ΔV%, and base moment ΔM%.

Fig. 8 shows the optimization of the TMDs parameters for the seven chimneys, in terms of top displacement, base shear, and base moment. The response parameters are plotted versus the mass ratio of the TMD. Once the average trends are detected for each chimney, the mass ratios optimizing the sizes of the TMDs are estimated. The optimal ratio should minimize the mass of the TMD and maximize the reduction in the displacement, base shear, and base bending moment [10,44].

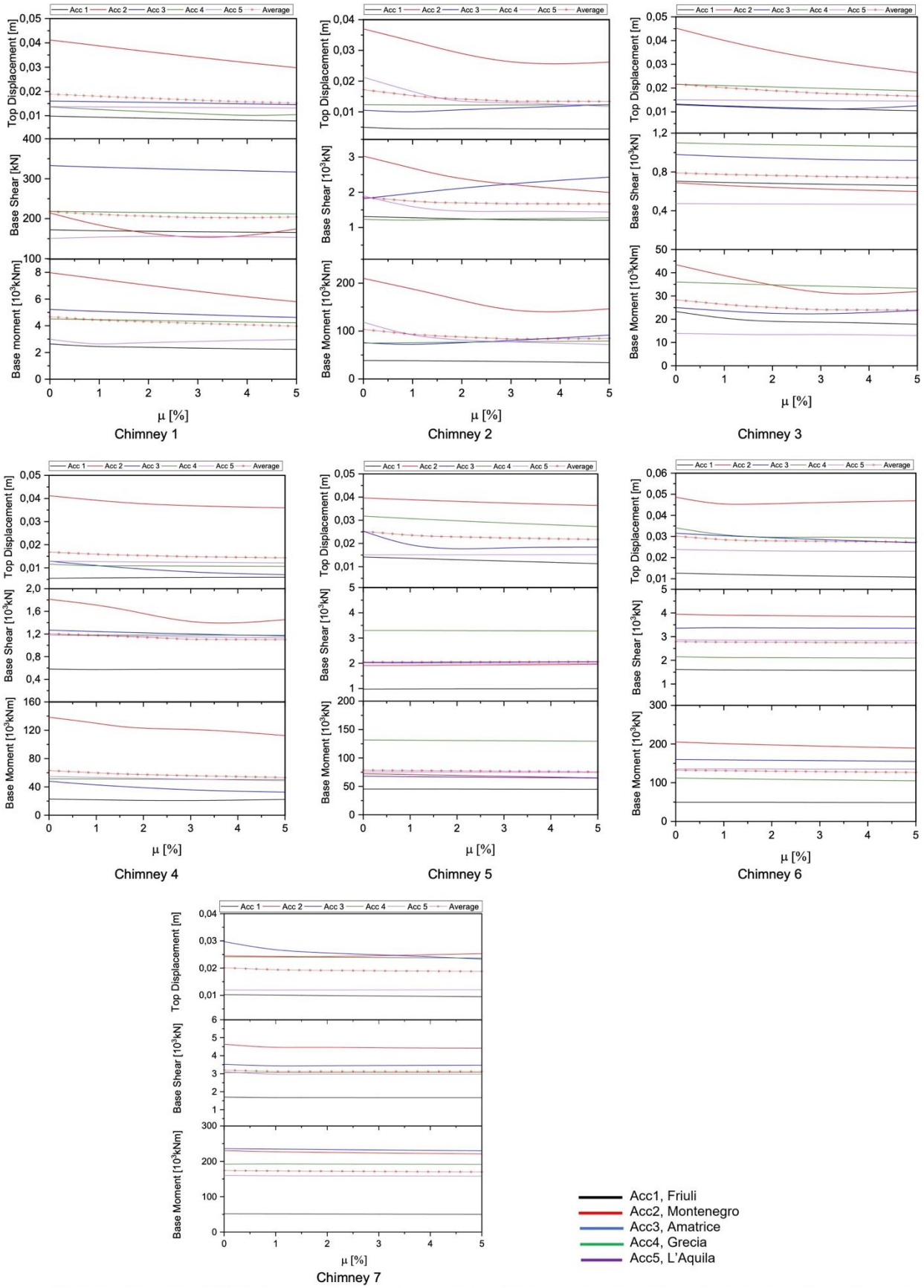


**Fig. 8.** Optimization of the TMDs parameters for the seven existing chimneys in terms of top displacement, base shear and base moment against the mass ratio (between the mass of the optimized TMD and the mass involved in the first and second vibrational modes).

For each chimney, the optimum mass ratio value ($\mu_{opt}$) is now known, as listed in Table 6. Once each optimum mass ratio ($\mu_{opt}$) is chosen, the parameters of each TMD are evaluated, in terms of horizontal stiffness ($k_{tmd}$), damping coefficient ($c_{tmd}$), by using Eqs. 1-5 (Table 6). For a complete definition of the mass-ratio percentages indicated in Table 6 as optimum mass ratios, these values are compared with those of the masses involved in systems characterized by chimneys with TMDs. For each system "chimney with TMD", Table 7 shows:

- The generalized mass, [62];
- The mass involved in the main vibrational modes (first and second modes);
- The weight and the mass of the optimized TMD;
- The weight of the TMD in comparison to the total weight of the chimney (given by the ratio TMD/W) expressed in percentage terms;
- the mass of the optimized TMD in relation to the Generalized mass (given by the ratio TMD / Generalized) expressed in percentage terms;
- the mass of the optimized TMD in relation to the mass involved in the first and second vibrational modes (given by the ratio TMD/V.Modal) expressed in percentage terms. The ratio TMD/V.Modal corresponds to the percentage already shown in Table 6 as the optimum mass ratio.

Table 6. Properties of the optimum TMDs selected for the seven chimneys (CH_1 to CH_7).

| Optimum TMD Properties | Chimney | | | | | | |
|---|---|---|---|---|---|---|---|
| | CH_1 | CH_2 | CH_3 | CH_4 | CH_5 | CH_6 | CH_7 |
| $\mu_{opt}$ | 4% | 3% | 3% | 3% | 3% | 5% | 3% |
| $\omega_{tmd}$ | 0.58 | 0.76 | 0.54 | 0.72 | 0.38 | 0.29 | 0.26 |
| $m_{tmd}$ [t] | 22.19 | 97.1 | 53.17 | 88.96 | 148.81 | 344.61 | 233.33 |
| $k_{tmd}$ [kN/m] | 293.22 | 2224.90 | 613.50 | 1812.41 | 828.56 | 1148.62 | 589.11 |
| $c_{tmd}$ [kNs/m] | 20.47 | 52.56 | 40.00 | 88.92 | 77.77 | 177.43 | 82.11 |

Table 7. Optimum mass ratio in comparison to the masses of the systems "chimneys with TMDs".

| Chimney | W (Total Weight) [kN] | Generalized Mass [kN/g] | I–II Vibration Modal, V.modal Mass [kN] | Optimal TMD [kN] | Optimal TMD [kN/g] | TMD/ W [%] | TMD/Generalized Mass [%] | TMD/V. Modal Mass [%] ≡ $\mu_{opt}$ (Table 6) |
|---|---|---|---|---|---|---|---|---|
| CH_1 | 9302 | 192.6 | 5439.9 | 217.6 | 22.2 | 2.3 | 11.5 | 4.0 |
| CH_2 | 47704.2 | 1055.9 | 31728.4 | 951.9 | 97.1 | 2.0 | 9.2 | 3.0 |
| CH_3 | 32041.7 | 546.5 | 17379.3 | 521.4 | 53.2 | 1.6 | 9.7 | 3.0 |
| CH_4 | 45564.3 | 1089.0 | 29078.5 | 872.4 | 89.0 | 1.9 | 8.2 | 3.0 |
| CH_5 | 90299.1 | 1466.3 | 48641.1 | 1459.2 | 148.8 | 1.6 | 10.1 | 3.0 |
| CH_6 | 140752 | 1647.0 | 67585.5 | 3379.3 | 344.6 | 2.4 | 20.9 | 5.0 |
| CH_7 | 168617 | 2926.2 | 76266.3 | 2288.0 | 233.3 | 1.4 | 8.0 | 3.0 |

Among all geometrical features, the slenderness ratio seems to control the size (mass ratio) of the TMD. The higher the slenderness ratio, the higher the optimum mass ratio of the TMD. For a slenderness ratio around $\lambda = 10$, the optimum mass ratio $\mu_{opt}$ is about 3%. However, for a higher slenderness ratio, for example $\lambda_{CH\_6} = 13.75$, the optimum mass ratio $\mu_{opt\ -CH\_6} = 5\%$. Also for $\lambda_{CH\_2} = 6.21$ the optimum mass ratio is $\mu_{opt\text{-}CH\_2} = 1.5\%$. Similar considerations may not be valid about the effect of the taper ratio $t_d$ on the size of the TMD, because chimneys with different $t_d$,

as CH_1 with $t_d = 0.52$ and CH_4 with $t_d = 0.99$, are characterized by very close mass ratio values (e.g. $\mu_{opt\text{-}CH\_1} = 4\%$ and $\mu_{opt\text{-}CH\_4} = 3\%$).

In Fig. 9, the frequency corresponding to the main vibrational modes of the chimney (value A) is split into two frequency values (values B and B'), corresponding to the first and the second vibrational modes of the system "chimney with TMD". It is worth mentioning that the values B and B' indicate vibrational modes in which only the mass of the TMD is involved, whereas the mass of the chimney participation to these modes is practically zero. Therefore, the first vibrational mode prevails that the mass of the chimney with almost zero mass of the TMD involved – in the system "chimney with TMD" – corresponds to higher frequency values (value C), (Table 8). In fact, value C corresponds to the frequency of the first vibrational mode of the system "chimney with TMD" in which the mass of the chimney is mostly involved because the mass of the TMD is substantially not involved.

Table 9 lists the controlled (with TMD) and uncontrolled responses, and the corresponding reductions (+ve) under the five different ground motions. The most important response reduction achieved by the TMDs is the top displacement. The base shear reductions under the five strong seismic events are not significant, in comparison to the displacement and base moment reductions.
The contribution of the TMD having the parameters shown in Table 6 is also evaluated for each chimney in the frequency domain by adopting the Fast Fourier Transform (FFT) of the five seismic time histories. In fact, in the FFT it is possible to detect the frequency of the chimney without TMD and the frequencies of the system given by the chimney equipped with the TMD. The effectiveness of the TMD on the seismic response depends on the properties of the structure and the characteristics of the earthquake. If the frequency of the only chimney intercepts the peaks of the FFT of the seismic input, the contribution of the TMD is much evident. Moreover, if the frequencies of the system "chimney with TMD" intercept the FFT of the seismic input in smoothed branches the effect of the TMD should be more profitable. By the FFT diagrams, the energetic approach (already described in Section 1) is evident because the TMD increases the mass and the damping of the new system "chimney with TMD", consequently the variation of vibrational mode shapes occurs in terms of participated mass and frequency values. The contribution of the TMD is well defined in the first and second vibrational modes where the generic system "chimney with TMD" has frequency values close to the one characterizing the chimney without TMD, but the damper mass is predominant in these modes, although the mass of the chimney is little involved.

Table 8. Mass of the TMD involved in the vibrational mode shapes of the system "chimney with TMD". The values called A, B, B' and C correspond to the ones shown in Fig. 9.

| value | case – CHIMNEY 1 | mode | mass of the TMD [%] |
|---|---|---|---|
| A | only chimney | Main frequency (modes I-II) | 0 |
| B | chimney with TMD | Main frequency (modes I-II) | 70 |
| B' | chimney with TMD | Main frequency (modes I-II) | 70 |
| C | chimney with TMD | First mode prevailing the mass of the chimney | 5 – (95%, mass of chimney 1) |

| value | case – CHIMNEY 2 | mode | mass of the TMD [%] |
|---|---|---|---|
| A | only chimney | Main frequency (modes I-II) | 0 |
| B | chimney with TMD | Main frequency (modes I-II) | 88 |
| B' | chimney with TMD | Main frequency (modes I-II) | 75 |
| C | chimney with TMD | First mode prevailing the mass of the chimney | 5 – (95%, mass of chimney 2) |

| value | case – CHIMNEY 3 | mode | mass of the TMD [%] |
|---|---|---|---|
| A | only chimney | Main frequency (modes I-II) | 0 |
| B | chimney with TMD | Main frequency (modes I-II) | 84 |
| B' | chimney with TMD | Main frequency (modes I-II) | 72 |
| C | chimney with TMD | First mode prevailing the mass of the chimney | 5 – (95%, mass of chimney 3) |

| value | case – CHIMNEY 4 | mode | mass of the TMD [%] |
|---|---|---|---|
| A | only chimney | Main frequency (modes I-II) | 0 |
| B | chimney with TMD | Main frequency (modes I-II) | 89 |
| B' | chimney with TMD | Main frequency (modes I-II) | 75 |
| C | chimney with TMD | First mode prevailing the mass of the chimney | 3 – (97%, mass of chimney 4) |

| value | case – CHIMNEY 5 | mode | mass of the TMD [%] |
|---|---|---|---|
| A | only chimney | Main frequency (modes I-II) | 0 |
| B | chimney with TMD | Main frequency (modes I-II) | 83 |
| B' | chimney with TMD | Main frequency (modes I-II) | 86 |
| C | chimney with TMD | First mode prevailing the mass of the chimney | 4 – (96%, mass of chimney 5) |

| value | case – CHIMNEY 6 | mode | mass of the TMD [%] |
|---|---|---|---|
| A | only chimney | Main frequency (modes I-II) | 0 |
| B | chimney with TMD | Main frequency (modes I-II) | 80 |
| B' | chimney with TMD | Main frequency (modes I-II) | 66 |
| C | chimney with TMD | First mode prevailing the mass of the chimney | 25 – (75%, mass of chimney 6) |

| value | case – CHIMNEY 7 | mode | mass of the TMD [%] |
|---|---|---|---|
| A | only chimney | Main frequency (modes I-II) | 0 |
| B | chimney with TMD | Main frequency (modes I-II) | 83 |
| B' | chimney with TMD | Main frequency (modes I-II) | 72 |
| C | chimney with TMD | First mode prevailing the mass of the chimney | 6 – (94%, mass of chimney 7) |

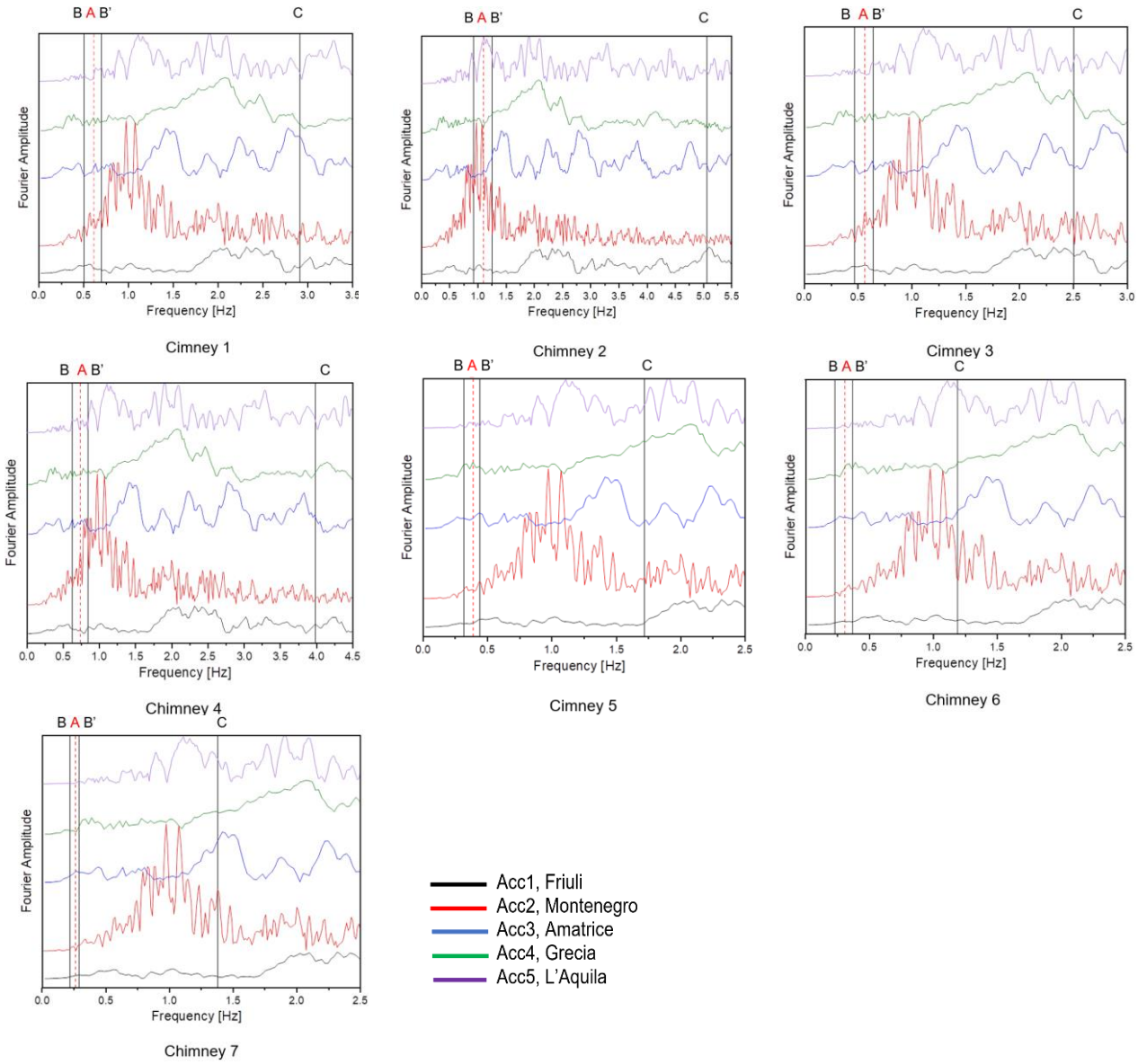


**Fig. 9.** Fourier amplitude of the seismic events in relation to the frequencies. Note: A = main frequency of the chimney without TMD; B and B' = first and second frequencies of chimney with TMD, C = frequency of the first mode where the mass of the chimney is predominant in the system "chimney with TMD"**.**

Table 9. Controlled (with TMD) and uncontrolled responses and corresponding reductions (+ve) under five different ground motions.

| | | Top Displacement (η) [m] | | | Base Shear (V) [kN] | | | Base Moment (M) [kN.m] | | |
|---|---|---|---|---|---|---|---|---|---|---|
| **CHIMNEY 1** $\mu_{opt}$ **4%** | Acc | No TMD | Opt. TMD | Δη [%] | No TMD | Opt. TMD | ΔV [%] | No TMD | Opt. TMD | ΔM [%] |
| | 1 | 0.0098 | 0.0081 | 16.7 | 172.2 | 166.2 | 3.5 | 2643.3 | 2274.7 | 13.9 |
| | 2 | 0.0411 | 0.0318 | 22.7 | 214.4 | 158.1 | 26.3 | 7976.5 | 6169.1 | 22.7 |
| | 3 | 0.0136 | 0.0101 | 25.3 | 333.0 | 319.7 | 4.0 | 5220.2 | 4726.2 | 9.5 |
| | 4 | 0.0160 | 0.0148 | 7.3 | 218.3 | 213.0 | 2.4 | 4513.6 | 4280.1 | 5.2 |
| | 5 | 0.0137 | 0.0133 | 3.4 | 150.4 | 154.7 | -2.9 | 2996.4 | 2908.4 | 2.9 |
| | | **Top Displacement (η) [m]** | | | **Base Shear (V) [kN]** | | | **Base Moment (M) [kN.m]** | | |
| **CHIMNEY 2** $\mu_{opt}$ **=1.5%** | Acc | No TMD | Opt. TMD | Δη [%] | No TMD | Opt. TMD | ΔV [%] | No TMD | Opt. TMD | ΔM [%] |
| | 1 | 0.0049 | 0.0045 | 9.3 | 1312.6 | 1261.2 | 3.9 | 38409.0 | 37842.6 | 1.5 |
| | 2 | 0.0370 | 0.0309 | 16.5 | 3027.1 | 2515.9 | 16.9 | 209828.1 | 176026.7 | 16.1 |
| | 3 | 0.0105 | 0.0103 | 2.0 | 1818.1 | 2044.4 | -12.4 | 75565.6 | 73724.5 | 2.4 |
| | 4 | 0.0123 | 0.0122 | 0.9 | 1230.2 | 1217.6 | 1.0 | 74694.5 | 76236.8 | -2.1 |
| | 5 | 0.0212 | 0.0146 | 31.2 | 1897.8 | 1504.1 | 20.7 | 118556.0 | 85166.5 | 28.2 |
| | | **Top Displacement (η) [m]** | | | **Base Shear (V) [kN]** | | | **Base Moment (M) [kN.m]** | | |
| **CHIMNEY 3** $\mu_{opt}$ **=3%** | Acc | No TMD | Opt. TMD | Δη [%] | No TMD | Opt. TMD | ΔV [%] | No TMD | Opt. TMD | ΔM [%] |
| | 1 | 0.0132 | 0.0113 | 14.4 | 704.9 | 674.1 | 4.4 | 23306.6 | 18757.1 | 19.5 |
| | 2 | 0.0452 | 0.0320 | 29.4 | 689.0 | 624.1 | 9.4 | 43444.7 | 31562.1 | 27.4 |
| | 3 | 0.0130 | 0.0111 | 14.3 | 980.2 | 930.1 | 5.1 | 25014.4 | 22342.0 | 10.7 |
| | 4 | 0.0216 | 0.0199 | 7.8 | 1100.6 | 1074.5 | 2.4 | 35997.7 | 34264.0 | 4.8 |
| | 5 | 0.0151 | 0.0147 | 2.3 | 474.4 | 468.5 | 1.2 | 13920.9 | 13441.2 | 3.4 |
| | | **Top Displacement (η) [m]** | | | **Base Shear (V) [kN]** | | | **Base Moment (M) [kN.m]** | | |
| **CHIMNEY 4** $\mu_{opt}$ **=3%** | Acc | No TMD | Opt. TMD | Δη [%] | No TMD | Opt. TMD | ΔV [%] | No TMD | Opt. TMD | ΔM [%] |
| | 1 | 0.0055 | 0.0059 | -7.5 | 581.5 | 576.4 | 0.9 | 22780.3 | 20816.1 | 8.6 |
| | 2 | 0.0412 | 0.0369 | 10.6 | 1811.9 | 1420.5 | 21.6 | 138448.0 | 121066 | 12.6 |
| | 3 | 0.0129 | 0.0082 | 36.3 | 1267.5 | 1200.7 | 5.3 | 47996.8 | 35862.1 | 25.3 |
| | 4 | 0.0116 | 0.0108 | 7.3 | 1182.9 | 1180.4 | 0.2 | 51342.2 | 50683.6 | 1.3 |
| | 5 | 0.0128 | 0.0124 | 3.4 | 1183.7 | 1148.3 | 3.0 | 54837.9 | 50837.4 | 7.3 |
| | | **Top Displacement (η) [m]** | | | **Base Shear (V) [kN]** | | | **Base Moment (M) [kN.m]** | | |
| **CHIMNEY 5** $\mu_{opt}$ **=3%** | Acc | No TMD | Opt. TMD | Δη [%] | No TMD | Opt. TMD | ΔV [%] | No TMD | Opt. TMD | ΔM [%] |
| | 1 | 0.014 | 0.012 | 12.3 | 976.9 | 990.2 | -1.4 | 45315.8 | 45050.6 | 0.6 |
| | 2 | 0.040 | 0.037 | 5.4 | 1914.5 | 1940.7 | -1.4 | 72106.9 | 67780.8 | 6.0 |
| | 3 | 0.025 | 0.018 | 28.5 | 2032.1 | 2047.5 | -0.8 | 67962.8 | 65940.1 | 3.0 |
| | 4 | 0.032 | 0.029 | 9.1 | 3298.1 | 3287.2 | 0.3 | 131700.3 | 130286.5 | 1.1 |
| | 5 | 0.015 | 0.015 | -0.3 | 2014.3 | 2002.5 | 0.6 | 75425.9 | 74928.9 | 0.7 |
| | | **Top Displacement (η) [m]** | | | **Base Shear (V) [kN]** | | | **Base Moment (M) [k.Nm]** | | |
| **CHIMNEY 6** $\mu_{opt}$ **=5%** | Acc | No TMD | Opt. TMD | Δη [%] | No TMD | Opt. TMD | ΔV [%] | No TMD | Opt. TMD | ΔM [%] |
| | 1 | 0.0126 | 0.0107 | 15.1 | 1613.9 | 1572.8 | 2.5 | 49506.4 | 48749.3 | 1.5 |
| | 2 | 0.0487 | 0.0469 | 3.6 | 3943.4 | 3838.0 | 2.7 | 205267.2 | 189276.7 | 7.8 |
| | 3 | 0.0315 | 0.0270 | 14.3 | 3356.5 | 3353.9 | 0.1 | 159853.4 | 155242.8 | 2.9 |
| | 4 | 0.0341 | 0.0293 | 14.2 | 2155.0 | 2091.7 | 2.9 | 111854.8 | 105059.7 | 6.1 |
| | 5 | 0.0239 | 0.0230 | 3.4 | 2865.4 | 2822.8 | 1.5 | 135493.4 | 134995.3 | 0.4 |
| | | **Top Displacement (η) [m]** | | | **Base Shear (V) [kN]** | | | **Base Moment (M) [k.Nm]** | | |
| **CHIMNEY 7** $\mu_{opt}$ **= 3%** | Acc | No TMD | Opt. TMD | Δη [%] | No TMD | Opt. TMD | ΔV [%] | No TMD | Opt. TMD | ΔM [%] |
| | 1 | 0.0102 | 0.0097 | 4.8 | 1699.7 | 1669.5 | 1.8 | 51690.9 | 50628.4 | 2.1 |
| | 2 | 0.0244 | 0.0245 | -0.3 | 4638.9 | 4443.8 | 4.2 | 230476.7 | 223681.7 | 2.9 |
| | 3 | 0.0297 | 0.0248 | 16.3 | 3522.0 | 3451.8 | 2.0 | 235710.7 | 232061.6 | 1.5 |
| | 4 | 0.0241 | 0.0238 | 1.2 | 3058.0 | 3069.8 | -0.4 | 191886.2 | 191845.0 | 0.0 |
| | 5 | 0.0119 | 0.0120 | -0.4 | 3110.4 | 2969.3 | 4.5 | 160012.2 | 158594.6 | 0.9 |

## 6. Equivalent damping (Phase C)

The contribution of the TMD in terms of equivalent damping ($\xi_e$) of chimney with TMD is assessed. The equivalent damping is evaluated by considering the system given by the chimney with TMD as single-degree-of-freedom (SDOF). For a SDOF under harmonic forces, it is possible to define the amplification factor [57] as the ratio between the top displacement of the chimney under the seismic action and the corresponding one under the harmonic force, here considered as a sinusoidal force. Each sinusoidal force has a frequency (f) included in the range $0.8 \cdot f_1 \leq f \leq 1.2 \cdot f_1$, where $f_1$ is the dominant frequency of each chimney. Therefore, it is possible to evaluate different amplification factors by considering the different seismic forces and sinusoidal forces with the frequencies included in the above-mentioned range. Consequently, several values of equivalent damping are evaluated as well for each chimney because the equivalent damping is given by the ratio between the unit and two times the amplification factor [57]. The equivalent damping values ($\xi_e$) obtained for each chimney equipped with TMD are plotted as a function of the main period (T) of each chimney without TMD in order to highlight the influence of T on the equivalent damping of the structure (Figure 10).
By considering the case studies here presented, the relation between the period and the equivalent damping is described by a curve characterized by the exponential law of Equation 6. This exponential law has the aim to underline how the efficiency of TMDs can be influenced by the vibrational features of the original structure.

$$\xi_e = 0.3178 \cdot e^{-\frac{T}{0.33685}} + 0.01809 + 0.0039T. \quad (6)$$

It is worth noting the influence of the main frequency of the chimney in the TMD contribution in terms of equivalent damping given to the main structure.

The equivalent damping due to the TMD under the five seismic events is not very significant. However, the effect of the TMDs in terms of frequencies variation is remarkable. The equivalent damping does not appear dependent on the individual properties of the chimneys. For high values of the geometrical slenderness, $\lambda_{CH\_1}$ = 12.5, $\lambda_{CH\_5}$ =11.66 and $\lambda_{CH\_6}$ =13.75, the equivalent damping values are similar. However, the equivalent damping due to the TMD depends on the characteristics of the seismic event combined with the natural frequency of the chimney. As shown in

Fig. **10**, the higher the natural frequency of the chimney, the higher the equivalent damping. In Fig. 10 the equivalent damping is dependent on the type of the seismic input (non-linear analysis). The equivalent damping is also dependent on the dominant period of the chimney. The higher the fundamental period, the lower the equivalent damping of the chimney with the TMD system. The five ground motions are as follows: Friuli (Acc1), Montenegro (Acc2), Amatrice (Acc3), Greece (Acc4), and L'Aquila (Acc5) (see also Fig. 7).

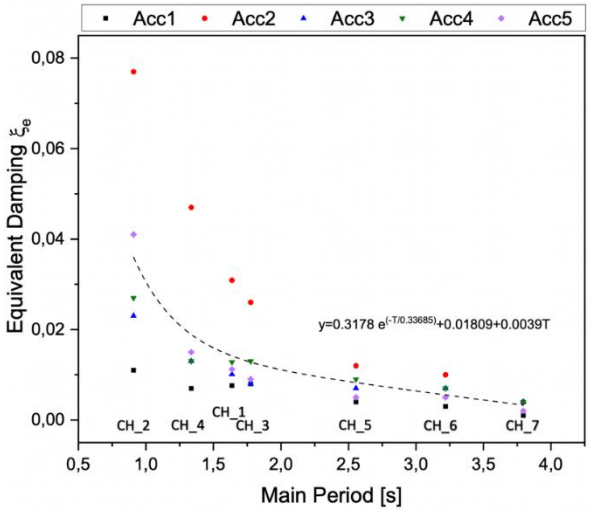


**Fig. 10.** Variation of the equivalent damping against the main periods of the seven chimneys.

## 7. Effect of chimney geometry on the performance of the TMD (Phase D)

This section aims to understand the dependence of the TMDs effectiveness on the chimneys geometrical parameters, particularly the slenderness ratio (λ) and the taper ratio ($t_d$). The capability of the TMDs to improve the seismic response of the chimneys is measured by three performance criteria. These criteria include the normalized base shear force (Ψ), the normalized base moment (Θ) and the normalized top displacement (Λ). The performance criteria are defined by referring to the height of the chimney (H) and the vertically distributed load ($q_h$), as follows. It is important to specify that $q_h$ is the additional load with respect to the self-weight. It considers the numbers of the internal pipes, floors, stairs, insulation, etc; $q_h$ values are obtained from the general description of the chimneys available in technical descriptions of the plants.

$$\Psi = \frac{V}{(H \cdot q_h)}, \tag{7}$$

$$\Theta = \frac{M}{(H^2 \cdot q_h)}, \tag{8}$$

$$\Lambda = \frac{\eta}{H}. \tag{9}$$

The performance criteria versus the slenderness ratio (λ) and the taper ratio ($t_d$) are shown in Figs. 13-14 for the chimneys with and without TMDs, under the five acceleration time histories. The normalized base shear (Ψ) and the normalized base moment (Θ) are influenced by the geometrical features of the chimney because their values significantly vary for chimneys having a different top height (H), geometrical slenderness (λ) and taper ratio (td). The normalized displacement may increase with the increase in the taper ratio (Fig. 11).
For Fig. 11, the taper ratio for each chimney is provided in Table 1. Chimney 2 (CH_2) has the lowest slenderness ratio (6.21), while chimney 6 (CH_6) has the highest slenderness ratio (13.75). The results for chimneys without TMDs are identified by the name of the earthquake and the type of the

analyses (e.g., Acc 1_nonlinear). The results for chimneys with TMDs are designated by the name of the earthquake, the type of the analyses and the presence of the TMD (e.g., Acc 1_nonlinearTMD).
However, the normalized top displacement does not show significant dependence on the taper ratio (Fig. 12). The results show that the higher the slenderness ratio ($\lambda_{CH\_1}$ = 12.50 and $\lambda_{CH\text{-}6}$ = 13.75), the lower the normalized base shear and base moment (Fig. 11). In contrast, the higher the taper ratio (td $_{CH\_4}$ = 0.99), the higher the normalized base shear and base moment (Fig. 12).
For Fig. 12, the taper ratio for each chimney is provided in Table 1. Chimney 1 (CH_1) and Chimney 4 (CH_4) have the lowest (0.52) and highest (0.99) taper ratio, respectively. The results for chimneys without TMDs are identified by the name of the earthquake and the type of the analyses (e.g., Acc 1_nonlinear). The results for chimneys with TMDs are designated by the name of the earthquake, the type of the analyses and the presence of the TMD (e.g., Acc 1_nonlinearTMD).

The TMD is more effective in reducing the base shear and moment for chimneys with a lower slenderness ratio. Nevertheless, the device shows superior performance in chimneys with a higher taper ratio. The efficacy of the TMD in reducing the top displacement is independent of the slenderness and taper ratios. This reveals that TMDs may reduce the top displacements of chimneys, regardless of their geometrical features. However, TMDs are more effective in reducing the base shear and moment in chimneys with lower slenderness ratio and higher taper ratio.

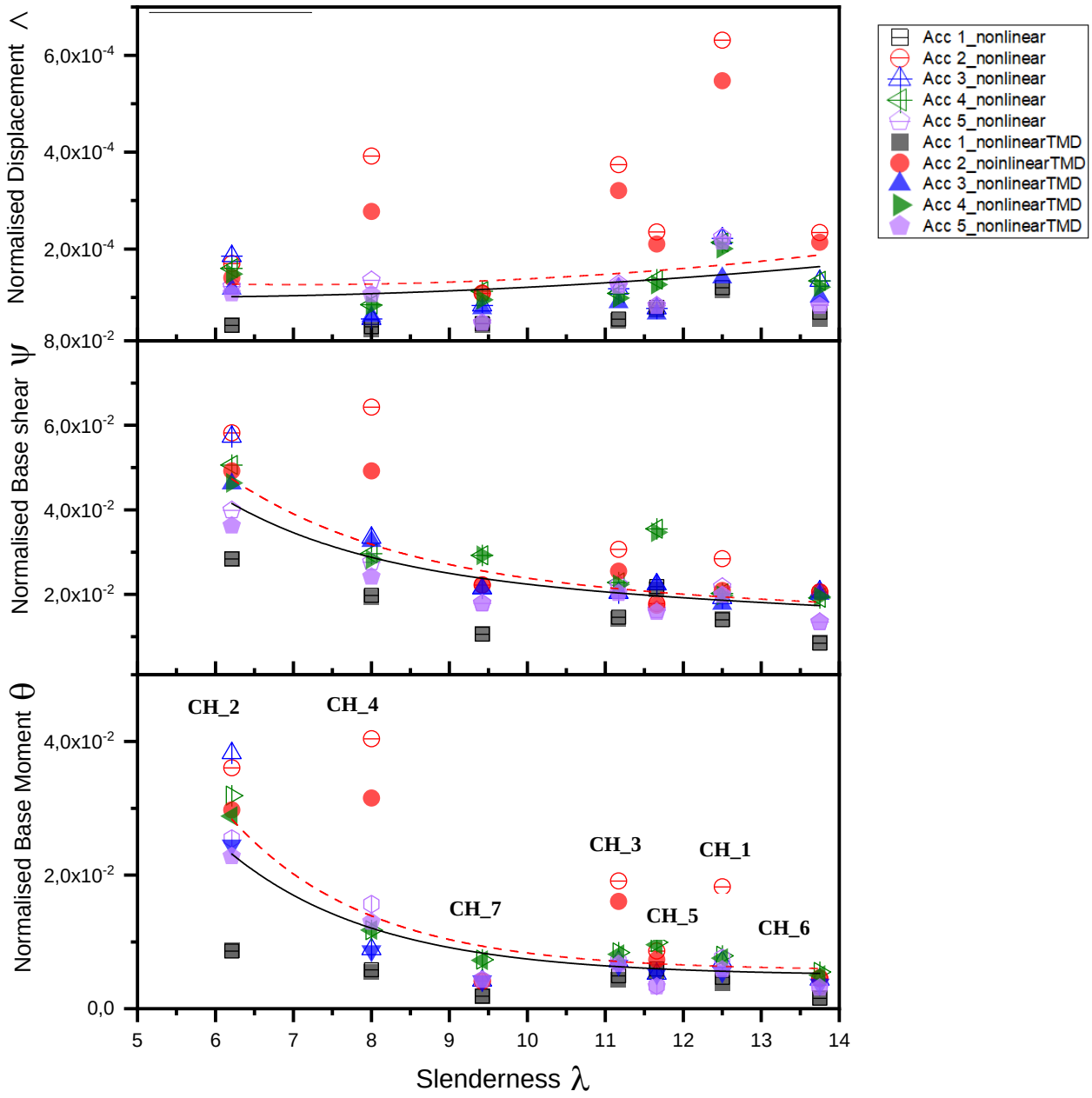


**Fig. 11.** Normalized response parameters (base shear, base moment and top displacement) versus the slenderness ratio.

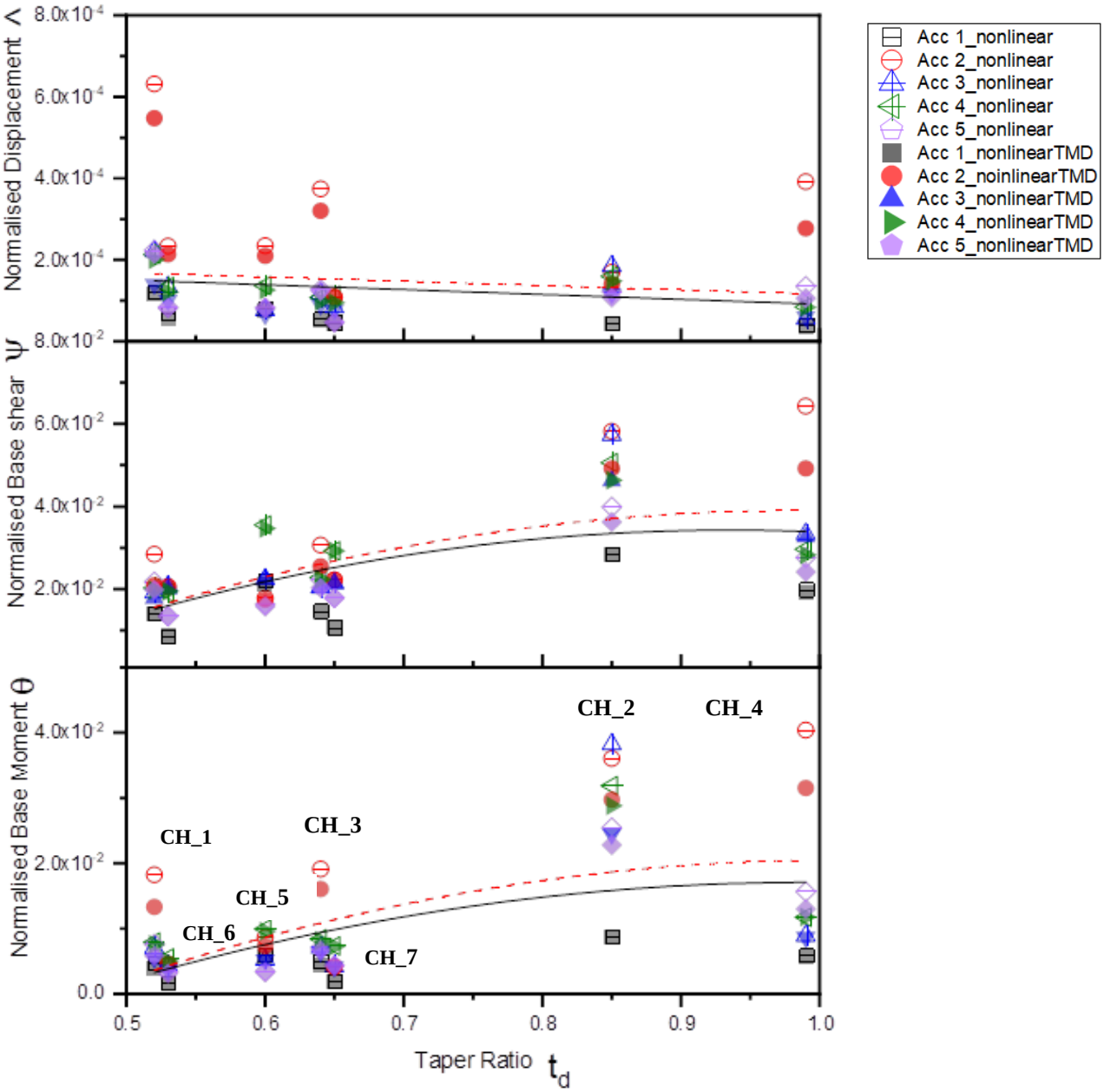


**Fig. 12.** Normalized response parameters (base shear, base moment and top displacement) versus the taper ratio.

## 8. Dissipated energy (Phase E)

We assumed that for a generic chimney case, the input energy ($E_i$) due to seismic action is the work done by the ground motion on the construction. Considering the time-dependent conservation of the energy, ($E_i$) is given by the summation of the kinetic energy ($E_k$), the elastic strain energy ($E_s$), the energy dissipated by the structure throughout the inelastic parameter ($E_h$), and the damped dissipative energy of the building and the TMD, when present ($E_d$). The formulations for calculating the input energy are available in the literature [63,64]. The energy dissipated by damping, under each seismic motion, for the seven chimneys, with and without TMDs, is evaluated.

In Fig. 13, the damping energy ($E_d$) is plotted for each chimney under five ground motions. The output of the energy analysis demonstrates the variation of the damping energy during the seismic events. The results are plotted in the time domain, for chimneys with and without TMDs. Each time history represents the percentage (ratio) of the damping energy against the input energy. Under the five earthquakes, the energy dissipated by damping, for the seven chimneys, increases when the TMD is installed. The contribution of energy dissipation by the TMD is more evident in the asymptotic part of the curves, especially under Acc 1 (Fruili, red lines) and Acc 2 (Montenegro, black lines).

In Fig. 14, the bar charts represent the maximum percentage of the kinetic energy ($E_k$), elastic strain energy ($E_s$), and the energy dissipated by the inelastic parameter ($E_h$), against the input energy (Ei), for all cases. While the TMD is generally increasing the energy dissipation by damping (Fig. 13), the other terms of energy (inelastic and kinetic energies) are generally reduced (Fig. 14).

In Fig. 14, the results are presented for chimneys without TMDs ($E_{h\_No\_TMD}$, $E_{k\_No\_TMD}$, and $E_{s\_No\_TMD}$), and chimneys with TMDs ($Eh_{\_TMD}$, $Ek_{\_TMD}$, and $Es_{\_TMD}$), under the five ground motions: Friuli (Acc1), Montenegro (Acc2), Amatrice (Acc3), Greece (Acc4), and L'Aquila (Acc5) as previously shown in Fig. 7. However, chimney 3 is a special case in which a different behavior is realized.

Under Acc2 and Acc4, the inelastic and kinetic energies increase with the installation of the TMD (Fig. 14). This could be a lack of proper tuning, in which the vibratory motion of the chimney is increased leading to higher kinetic and inelastic energies. Generally, a major part of the input energy is dissipated by damping (structural and TMD), and the remainder of the input energy is transformed to inelastic and kinetic energies, while the strain energy is close to zero. The presence of the TMD slightly reduces the kinetic energy (reduced vibrations).

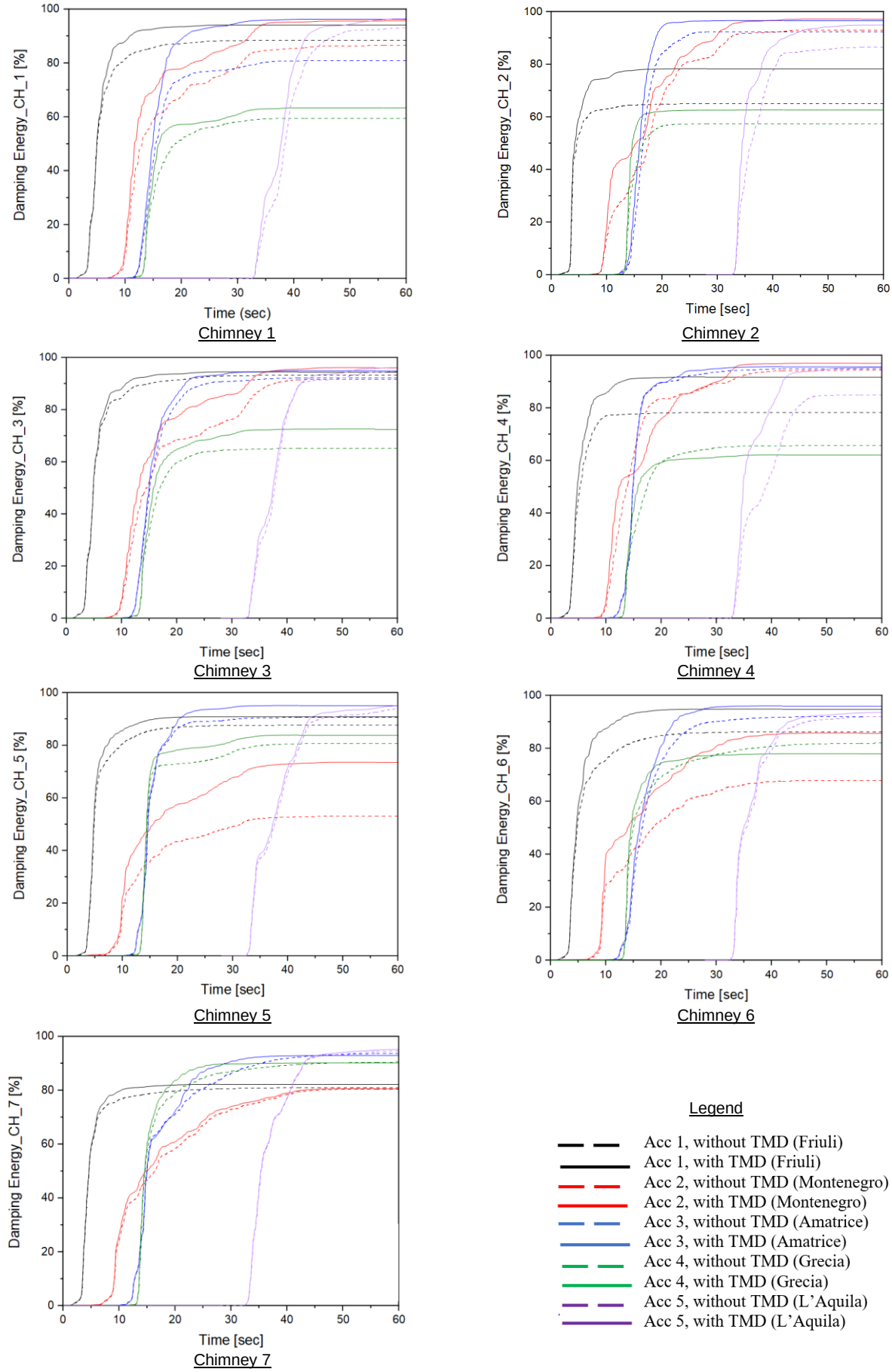


**Fig. 13.** Percentage of energy dissipated by damping ($E_d$) with respect to the total input energy ($E_i$).

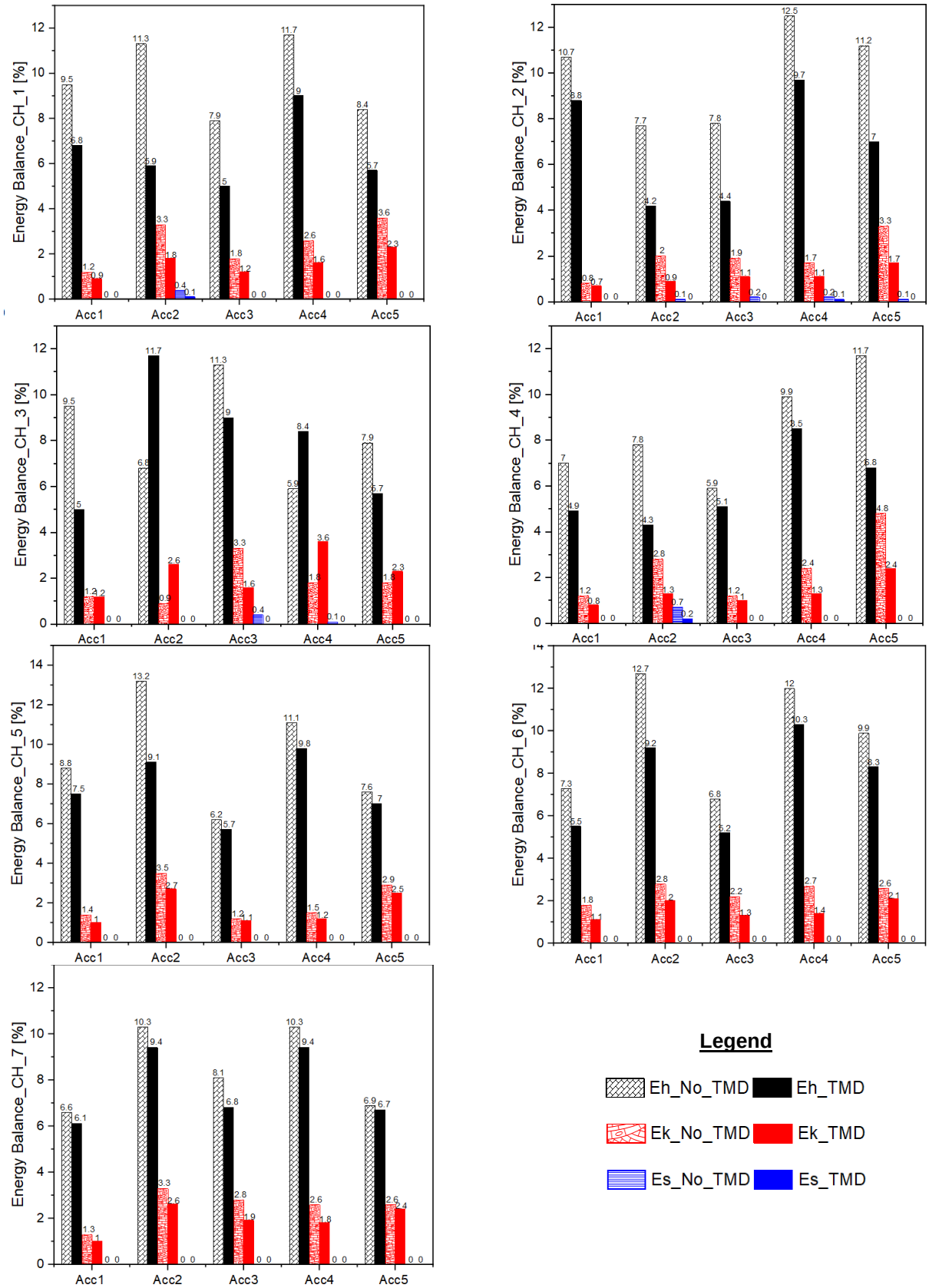


**Fig. 14.** Percentage variations of inelastic energy ($E_h$), kinetic energy ($E_k$) and elastic strain energy ($E_s$) with respect to the input energy ($E_i$) for the seven chimneys.

## 9. Conclusions

This paper has investigated the performance of TMDs in reducing the dynamic effects of earthquakes on seven RC chimneys originally designed for static and wind loads. The parameters of TMDs are optimized starting from the vibrational mode shapes of the chimneys and consequently the mass ratio, under the nonlinear properties of the chimneys. The capability of TMDs in reducing the top displacement, base shear, and base moment is assessed. The findings of the paper are as follows.

- The installation of the TMDs can change the mode shapes and the relative involved masses because a new structural system characterized by the chimney and the TMD is obtained. In the new system, the first vibrational modes generally involve the mass of the TMDs while the mass of the chimney substantially remains not involved; the mass of the chimney begins to be predominantly involved in vibrating modes characterized by frequencies that do not negatively affect the seismic response of the system.
- The mass ratio of the TMD is dependent on the geometrical slenderness of the chimney. For a low slenderness ratio (i.e., 6.2), the optimum mass ratio of the TMD is about 1.5%. A chimney with higher slenderness demands a higher mass ratio of the TMD. For a slenderness ratio of about 10, the optimum TMD mass ratio is about 3%, whereas, for higher slenderness ratios (i.e., 12.5 to 14), the optimum TMD mass ratio is close to 5%.
- In contrast with the slenderness ratio, the mass ratio of the TMD is insensitive to the geometrical taper ratio of the chimney.
- For the seismic records considered in the current study, the dominant benefit of the TMD is a reduction in the top displacement of the chimney.
- The normalized base shear and moment are sensitive to the geometrical features of the chimneys, especially the slenderness and the taper ratios. However, the normalized top displacement is less sensitive to the geometrical characteristics of the chimneys (slenderness and taper ratios)
- The TMD is more effective in reducing the base shear and base moment for chimneys with a lower slenderness ratio. The efficacy of the TMD in reducing the top displacement is independent of the slenderness and taper ratios. This reveals that TMDs may reduce the top displacements of chimneys, regardless of their geometrical features.
- The equivalent damping achieved by the TMD depends on the frequency of the chimney and the seismic record. The effect of the TMDs in terms of frequencies variation is remarkable. The equivalent damping is less independent of other parameters of the chimney, such as the taper ratio, even when the slenderness ratio is more influential. For high values of geometrical slenderness ($\lambda=11\div14$), the equivalent damping values are similar.
- The energy balance study reveals higher damping energy for the case of chimneys with TMDs. The contribution is much evident in the asymptotic branch of the energy curves. The damping energy increases with the TMDs, while the kinetic and inelastic energies decrease, even when the strain energy contribution is close to zero.
- Overall, the current study shows that Tuned Mass Dampers (TMDs) are applicable for RC chimneys, to support the industrial developments and environmental requirements. TMDs support the current call for sustainability to improve resilience and hence the structural ability to survive under environmental conditions.

## Compliance with ethical standards

Conflict of Interest: The authors declare that they have no conflict of interest.

## Reference

[1] Bayraktar A, Çalik İ, Türker T, Ashour A. Restoration effects on experimental dynamic characteristics of masonry stone minarets. Mater Struct 2018;51:1–14.
[2] Breccolotti M, Materazzi AL. The role of the vertical acceleration component in the seismic response of masonry chimneys. Mater Struct 2016;49:29–44.
[3] Pallarés FJ, Agüero A, Martín M. Seismic behaviour of industrial masonry chimneys. Int J Solids Struct 2006. https://doi.org/10.1016/j.ijsolstr.2005.06.014.
[4] Longarini N, Zucca M, Silvestro G. The constructions vibration control by tuned mass dumper. IABSE Conf. Geneva 2015 Struct. Eng. Provid. Solut. to Glob. Challenges - Rep., 2015.
[5] Pallarés FJ, Agüero A, Ivorra S. A comparison of different failure criteria in a numerical seismic assessment of an industrial brickwork chimney. Mater Struct 2009;42:213–26.
[6] Golewski GL. On the special construction and materials conditions reducing the negative impact of vibrations on concrete structures. Mater Today Proc 2021;45. https://doi.org/10.1016/j.matpr.2021.01.031.
[7] DIVER M. CALCUL PRATIQUE DES CHEMINEES EN BETON ARME. Inst Tech Batim Des Trav Publics-Annales 1969.
[8] NTC2018. Norme Tecniche per le Costruzioni. 2018.
[9] Elias S, Matsagar V, Datta TK. Distributed Multiple Tuned Mass Dampers for Wind Response Control of Chimney with Flexible Foundation. Procedia Eng., 2017. https://doi.org/10.1016/j.proeng.2017.09.087.
[10] Elias S, Matsagar V. Research developments in vibration control of structures using passive tuned mass dampers. Annu Rev Control 2017. https://doi.org/10.1016/j.arcontrol.2017.09.015.
[11] Elias S, Rupakhety R, Ólafsson S. Tuned Mass Dampers for Response Reduction of a Reinforced Concrete Chimney Under Near-Fault Pulse-Like Ground Motions. Front Built Environ 2020. https://doi.org/10.3389/fbuil.2020.00092.
[12] Elias S, Matsagar V, Datta TK. Effectiveness of distributed tuned mass dampers for multi-mode control of chimney under earthquakes. Eng Struct 2016. https://doi.org/10.1016/j.engstruct.2016.06.006.
[13] Longarini N, Cabras L, Zucca M, Chapain S, Aly AM. Structural Improvements for Tall Buildings under Wind Loads: Comparative Study. Shock Vib 2017;2017. https://doi.org/10.1155/2017/2031248.
[14] Wilson JL. Earthquake response of tall reinforced concrete chimneys. Eng Struct 2003. https://doi.org/10.1016/S0141-0296(02)00098-6.
[15] Wilson JL. The cyclic behaviour of reinforced concrete chimney sections with and without openings. Adv Struct Eng 2009. https://doi.org/10.1260/136943309788708329.
[16] Wang L, Fan X yan. Failure cases of high chimneys: A review. Eng Fail Anal 2019. https://doi.org/10.1016/j.engfailanal.2019.07.032.
[17] Golewski GL. Physical characteristics of concrete, essential in design of fracture-resistant, dynamically loaded reinforced concrete structures. Mater Des Process Commun 2019;1. https://doi.org/10.1002/mdp2.82.
[18] Golewski GL. Validation of the favorable quantity of fly ash in concrete and analysis of crack propagation and its length – Using the crack tip tracking (CTT) method – In the fracture toughness examinations under Mode II, through digital image correlation. Constr Build Mater 2021;296:122362. https://doi.org/https://doi.org/10.1016/j.conbuildmat.2021.122362.
[19] Golewski GL. Evaluation of fracture processes under shear with the use of DIC technique in fly ash concrete and accurate measurement of crack path lengths with the use of a new crack tip tracking method. Measurement 2021;181:109632. https://doi.org/https://doi.org/10.1016/j.measurement.2021.109632.
[20] Gil D, Golewski GL. Effect of Silica Fume and Siliceous Fly Ash Addition on the Fracture

Toughness of Plain Concrete in Mode I. IOP Conf Ser Mater Sci Eng 2018;416:12065. https://doi.org/10.1088/1757-899X/416/1/012065.
[21] Golewski GL. An Analysis of Fracture Toughness in Concrete with Fly Ash Addition, Considering all Models of Cracking. IOP Conf Ser Mater Sci Eng 2018;416:12029. https://doi.org/10.1088/1757-899X/416/1/012029.
[22] Bońkowski PA, Zembaty Z, Minch MY. Seismic effects on leaning slender structures and tall buildings. Eng Struct 2019. https://doi.org/10.1016/j.engstruct.2019.109518.
[23] Tabeshpour MR. Nonlinear dynamic analysis of chimney-like towers. Asian J Civ Eng 2012.
[24] Bońkowski P, Zembaty Z, Minch MY. Nonlinear interaction of initial leaning of r/c slender tower with its seismic response. Insights Innov. Struct. Eng. Mech. Comput. - Proc. 6th Int. Conf. Struct. Eng. Mech. Comput. SEMC 2016, 2016. https://doi.org/10.1201/9781315641645-50.
[25] N L, Pandian GAM. Effect of Dynamic Loads on Tall RCC Chimneys of Different Heights with Elliptical and Circular Cross sections. IOSR J Mech Civ Eng 2014. https://doi.org/10.9790/1684-11416367.
[26] Akyürek O, Suksawang N, Go TH, Tekeli H. Performance evaluation of a reinforced concrete building strengthened respectively by the infill wall, active and passive tuned mass damper under seismic load. Comput Struct 2019. https://doi.org/10.1016/j.compstruc.2019.07.006.
[27] Saffari A, Ataei M, Sereshki F, Naderi M. Environmental impact assessment (EIA) by using the Fuzzy Delphi Folchi (FDF) method (case study: Shahrood cement plant, Iran). Environ Dev Sustain 2019;21:817–60.
[28] Ali TKM. Shear strength of a reinforced concrete beam by PET fiber. Environ Dev Sustain 2021;23:8433–50.
[29] Zerva A, Grigoroudis E, Karasmanaki E, Tsantopoulos G. Multiple criteria analysis of citizens' information and trust in climate change actions. Environ Dev Sustain 2021;23:7706–27.
[30] Tembhare SP, Bhanvase BA, Barai DP, Dhoble SJ. E-waste recycling practices: a review on environmental concerns, remediation and technological developments with a focus on printed circuit boards. Environ Dev Sustain 2021:1–83.
[31] Miranda JC. Analytical parameters for equal mode damping ratio inducing TMDs for seismic response reduction. Bull Earthq Eng 2021;19:263–85.
[32] Kazemi F, Miari M, Jankowski R. Investigating the effects of structural pounding on the seismic performance of adjacent RC and steel MRFs. Bull Earthq Eng 2021;19:317–43.
[33] Faiella D, Mele E. Vibration characteristics and higher mode coupling in intermediate isolation systems (IIS): a parametric analysis. Bull Earthq Eng 2019;17:4347–87.
[34] Puthanpurayil AM, Lavan O, Carr AJ, Dhakal RP. Elemental damping formulation: an alternative modelling of inherent damping in nonlinear dynamic analysis. Bull Earthq Eng 2016;14:2405–34.
[35] Ruiz R, Taflanidis AA, Lopez-Garcia D, Vetter CR. Life-cycle based design of mass dampers for the Chilean region and its application for the evaluation of the effectiveness of tuned liquid dampers with floating roof. Bull Earthq Eng 2016;14:943–70.
[36] Pu W, Liu C, Dai F. Optimum hysteretic damper design for multi-story timber structures represented by an improved pinching model. Bull Earthq Eng 2018;16:6221–41.
[37] Zhou Y, Aguaguiña M, Beskos DE, Gong S. A displacement-based seismic design method for building structures with nonlinear viscoelastic dampers. Bull Earthq Eng 2021:1–51.
[38] Matta E. Seismic effectiveness and robustness of tuned mass dampers versus nonlinear energy sinks in a lifecycle cost perspective. Bull Earthq Eng 2021;19:513–51.
[39] Zeng Y, Pan P, Guo Y. Development of distributed tunable friction pendulum system (DTFPS) for semi-active control of base-isolated buildings. Bull Earthq Eng 2021:1–26.
[40] Donà M, Bernardi E, Zonta A, Tan P, Zhou F. Evaluation of optimal FVDs for inter-storey

isolation systems based on surrogate performance models. Bull Earthq Eng 2021:1–35.
[41] Gill D, Elias S, Steinbrecher A, Schröder C, Matsagar V. Robustness of multi-mode control using tuned mass dampers for seismically excited structures. Bull Earthq Eng 2017;15:5579–603.
[42] Rakicevic ZT, Bogdanovic A, Jurukovski D, Nawrotzki P. Effectiveness of tune mass damper in the reduction of the seismic response of the structure. Bull Earthq Eng 2012;10:1049–73.
[43] Nuzzo I, Losanno D, Caterino N. Seismic design and retrofit of frame structures with hysteretic dampers: a simplified displacement-based procedure. Bull Earthq Eng 2019;17:2787–819.
[44] Longarini N, Zucca M. A chimney's seismic assessment by a tuned mass damper. Eng Struct 2014;79. https://doi.org/10.1016/j.engstruct.2014.05.020.
[45] Takewaki I. Building Control with Passive Dampers: Optimal Performance-based Design for Earthquakes. 2009. https://doi.org/10.1002/9780470824931.
[46] Kareem A, Kline S. Performance of Multiple Mass Dampers under Random Loading. J Struct Eng 1995. https://doi.org/10.1061/(asce)0733-9445(1995)121:2(348).
[47] Abé M, Fujino Y. Dynamic characterization of multiple tuned mass dampers and some design formulas. Earthq Eng Struct Dyn 1994. https://doi.org/10.1002/eqe.4290230802.
[48] Multitech. 41 t Tuned Mass Damper 2021.
[49] Guedes JM, Lopes V, Quelhas B, Costa A, Ilharco T, Coelho F. Brick masonry industrial chimneys: assessment, evaluation and intervention. Philos Trans R Soc A 2019;377:20190012.
[50] Midas. Midas GEN FX Program - General structure design system n.d.
[51] Park R, Kent DC, Sampson RA. REINFORCED CONCRETE MEMBERS WITH CYCLIC LOADING. ASCE J Struct Div 1972.
[52] Scott BD, Park R, Priestley MJN. STRESS-STRAIN BEHAVIOR OF CONCRETE CONFINED BY OVERLAPPING HOOPS AT LOW AND HIGH STRAIN RATES. J Am Concr Inst 1982. https://doi.org/10.14359/10875.
[53] Krack M. Nonlinear modal analysis of nonconservative systems: Extension of the periodic motion concept. Comput Struct 2015;154:59–71.
[54] Pesheck E, Boivin N, Pierre C, Shaw SW. Nonlinear modal analysis of structural systems using multi-mode invariant manifolds. Nonlinear Dyn 2001;25:183–205.
[55] Kerschen G, Peeters M, Golinval J-C, Stéphan C. Nonlinear modal analysis of a full-scale aircraft. J Aircr 2013;50:1409–19.
[56] Tsai H -C, Lin G -C. Optimum tuned-mass dampers for minimizing steady-state response of support-excited and damped systems. Earthq Eng Struct Dyn 1993. https://doi.org/10.1002/eqe.4290221104.
[57] Ormondroyd J, Den Hartog JP. The theory of the dynamic vibration absorber. Trans Am Soc Mech Eng 1928.
[58] Li C, Qu W. Optimum properties of multiple tuned mass dampers for reduction of translational and torsional response of structures subject to ground acceleration. Eng Struct 2006. https://doi.org/10.1016/j.engstruct.2005.09.003.
[59] Hoang N, Fujino Y, Warnitchai P. Optimal tuned mass damper for seismic applications and practical design formulas. Eng Struct 2008. https://doi.org/10.1016/j.engstruct.2007.05.007.
[60] Zucca M, Tropeano G, Erbì E, Crespi P. Evaluation of the seismic behavior of multi-propped shallow underground structures embedded in granular soils: A comparison between coupled and decoupled approaches. Earthq. Geotech. Eng. Prot. Dev. Environ. Constr. Proc. 7th Int. Conf. Earthq. Geotech. Eng. 2019, 2019.
[61] Zucca M, Valente M. On the limitations of decoupled approach for the seismic behaviour evaluation of shallow multi-propped underground structures embedded in granular soils. Eng Struct 2020. https://doi.org/10.1016/j.engstruct.2020.110497.

[62] Ewins D. Modal Testing: Theory and Practice. II. Wiley; 2009.
[63] Elias S. Seismic energy assessment of buildings with tuned vibration absorbers. Shock Vib 2018. https://doi.org/10.1155/2018/2051687.
[64] Anam I, Manju F, Khan F. Seismic vibration control of nonlinear RC structures. Wind Earthq. Eng. - Proc. 10th East Asia-Pacific Conf. Struct. Eng. Constr. EASEC 2010, 2006.